CHAPTER 2 - OBJECTIVES

LIQUID PHASE DIFFUSION BONDING OF NICKEL-BASE SUPERALLOY COMPONENTS USING NOVEL BRAZE FILLER METALS

2.1) Background

Turbine vanes or nozzles operating in power generation engines often develop wide cracks during service. When the engine is overhauled, or when cracks propagate to a specific length during service, a decision has to be made whether new replacement parts should be purchased, or whether the damaged components should be repaired at a fraction of the cost of a new part. On the basis of economic considerations, the majority of users opt for repair.

Many γ'-strengthened nickel-base superalloys are difficult to weld successfully and brazing techniques have gained prominence in the turbine repair industry in the last decades. Since conventional brazing techniques rely on capillary action to draw the molten braze filler metal into the joint gap, these processes are only suitable for repairing narrow cracks (less than 0.25 mm in width). In order to overcome this limitation, wide gap brazing techniques have been developed for repairing cracks up to 1 mm in width. At present these techniques are widely used in applications involving the repair of turbine components for aircraft engines, where wide cracks (more than 1 mm in width) are seldom encountered.

Conventional wide gap brazing techniques, however, find limited application in the repair of land-based turbine components, such as those found in power generation engines, where cracks widths often exceed 1 mm. When wide gap brazing techniques are applied to repair cracks wider than 1 mm, the repaired areas normally achieve only 60 to 70% of the mechanical properties of the base metal, and display a tendency for premature degradation and cracking in service. A need has therefore been identified for a reliable technique suitable for repairing the wide cracks often observed in land-based turbine engine components.

In the past most repair vendors operated independently from the original engine manufacturers (OEM's). As a result of the lucrative nature of the repair market, all the OEM's (including General Electric, Pratt & Whitney (P&W), Siemens and Alstom) have since opened their own repair shops or acquired some of the independent repair vendors. For the end user the most important deciding factor when choosing a repair vendor is often not the cost involved, but the technology utilized during the repair. In order to remain competitive in the repair business, repair vendors therefore have to develop, implement and market new repair techniques for refurbishing degraded turbine components on an ongoing basis.

2.2) Objectives of this investigation

The majority of commercially available Ni-base braze filler metals contain B and/or Si as melt point depressants, and display a tendency for forming brittle intermetallic phases (such as borides and silicides) within the braze joint when used to repair wide gaps. The objective of this investigation was to capitalize on the need for a reliable repair technique for wide cracks in land-based turbine components by developing novel braze filler metals which ensure high strength joints with good ductility when used in conjunction with the liquid sintering process to repair wide cracks. The investigation was designed to:

- evaluate the use of two novel melt point depressants, namely Hf and Zr, in Ni- and Co-base braze filler metals, and
- optimize the liquid phase diffusion bonding process in combination with these novel braze filler metals with the aim of producing high strength joints with good ductility and mechanical properties at elevated temperature approaching those of the base metal.

The results of this investigation are considered in more detail in the remainder of this document.

CHAPTER 3 - EXPERIMENT 1

MICROSTRUCTURAL EXAMINATION OF NOVEL BINARY EUTECTIC Ni-Hf AND Ni-Zr BRAZE ALLOYS

This chapter describes the results of a series of preliminary experiments aimed at determining whether hafnium and zirconium can be used as melt point depressants in novel Ni-base braze filler metals.

3.1) Introduction

Examination of binary phase diagrams with nickel as solvent revealed that hafnium and zirconium may be suitable for use as melt point depressants in novel braze filler metals for repairing Ni-base superalloys. Nash and Nash, as quoted in ASM Handbook [2], reported the existence of an invariant eutectic reaction in the Ni-Hf binary system at a composition of 30.5 wt.% Hf and 69.5 wt.% Ni (see **Figure 49**). The eutectic temperature was quoted as 1190°C. According to Nash and Jayanth, also quoted in ASM Handbook [2], the Ni-Zr binary system contains a eutectic point located at 13 wt.% Zr and 87 wt.% Ni (see **Figure 50**). The eutectic temperature was quoted as 1170°C. In order to determine whether Hf and Zr can be used as melt point depressants in Ni-base braze filler metals, nickel powder was mixed with hafnium powder or zirconium powder to make up the simple binary eutectic compositions obtained from the phase diagrams.

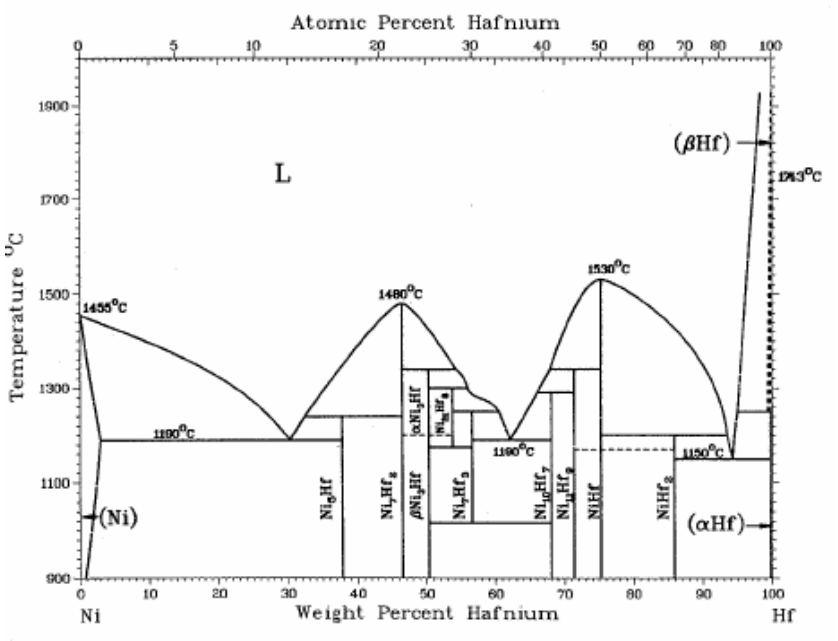

Figure 49 – Binary Ni-Hf phase diagram [2].

The objectives of Experiment 1 were therefore:

- to verify that eutectic Ni-Hf and Ni-Zr braze alloys melt and flow in the same way as the braze alloys currently used in the aerospace and land-based gas turbine repair industries,
- to determine the optimum braze temperatures for both alloys, and
- to examine the microstructures of the braze joints after relatively short brazing times (40 minutes), and to compare the joint microstructures with those obtained after extended times (18 hours) at the braze temperature.

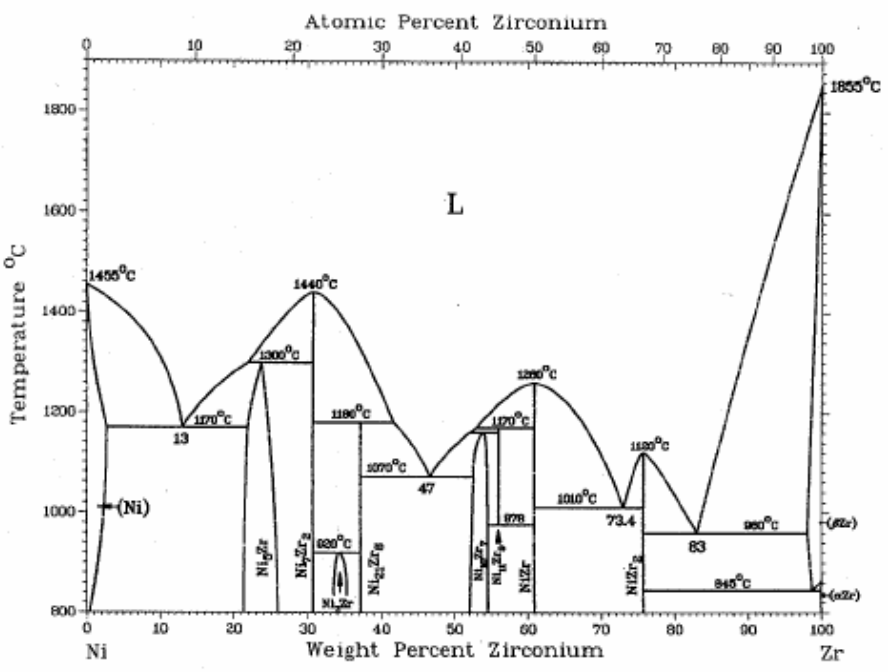

Figure 50 – Binary Ni-Zr phase diagram [2].

3.2) Experimental procedure

Inconel 738 (abbreviated as In738 throughout the remainder of this document), with the nominal chemical composition shown in Table 8, was used as parent metal during the course of this investigation. Flat plate was obtained by sectioning slabs of material from the root of scrap blades using Electric Discharge Machining (EDM). The root of a turbine blade is not exposed to appreciable temperatures or stresses in service, and material removed from this area is often viewed as virgin-like as-cast material. The In738 material was prepared for brazing by grinding to a thickness of 2 mm. The plates were mechanically cleaned by grit blasting with 220 grit silicon carbide media, and then wiped with acetone to remove any surface residue from the grit blasting process.

Table 8 – Nominal chemical composition of the In738 parent metal used during the course of this investigation (wt.%, balance nickel).

B	C	Co	Cr	Mo	Al	W	Ta	Nb	Ti	Zr
0.001	0.17	8.5	16	1.7	3.4	2.6	1.7	2.0	3.4	0.1

The novel Ni-Hf braze filler metal was prepared by mixing 69.5 wt.% Ni and 30.5 wt.% Hf (the eutectic composition) in powder form. The powder mixture was then mixed with a binder to form a braze paste. The Ni-Zr braze paste was produced in a similar way by mixing 87 wt.% Ni powder and 13 wt.% Zr powder with a binder. Following evaporation of the acetone from the In738 plates, a layer of Ni-Hf or Ni-Zr braze paste was applied over the In738 plate or between two In738 plates (like a filling in a sandwich). The samples were dried for an hour before being placed in a laboratory vacuum furnace with a maximum temperature capability of 1260°C. It should be noted that the vacuum furnace used in this investigation did not have any quench facilities. The samples were therefore slow cooled to room temperature in the furnace.

The vacuum braze cycle used for both braze alloys was as follows:

1) Ramp up to a temperature of 450°C at a minimum rate of 9°C/minute.
2) Hold at 450°C for 20 minutes to allow the binder to burn off.
3) Ramp up to a temperature of 1150°C at a minimum rate of 9°C/minute.
4) Hold at 1150°C for 20 minutes to allow the samples to stabilize at this temperature.
5) Ramp up to a temperature of 1190°C, 1214°C or 1238°C at a minimum rate of 9°C/minute to allow the Ni-Hf braze alloy to melt; or ramp up to a temperature of 1170°C, 1204°C or 1238°C to allow the Ni-Zr alloy to melt.
6) Hold at the braze temperature for 40 minutes or 18 hours.
7) Furnace cool to room temperature.

After exposing the samples to the vacuum brazing cycle described above, the brazed samples were sectioned and mounted in resin using conventional metallographic practices. The mounted samples were polished, etched with Marble's reagent to reveal the microstructure and examined using optical and scanning electron microscopy (SEM) techniques. A Nikon Epiphot 200 optical microscope with a maximum magnification of 1000X, and a JOEL-Oxford scanning electron microscope equipped with ZAF software correction, were used. The acceleration voltage was 20 kV, the % dead time approximately 50 seconds, the sample tilt angle 0°, and the total acquisition time 150 seconds.

3.3) Results and discussion

3.3.1 Optimization of the braze temperature:

Neither the Ni-Hf, nor the Ni-Zr braze, melted at their published eutectic temperatures of 1190°C and 1170°C, respectively. This could be as a result of experimental error, such as incorrect weighing of the Ni-Hf or Ni-Zr powders (unlikely), insufficient mixing (resulting in segregated braze powders), or inaccurate furnace calibration. It may also be due to insufficient thermodynamic driving force for melting as a result of the low levels of superheat above the equilibrium eutectic temperatures.

Since neither alloy melted at their published eutectic temperatures, the braze temperatures were raised to 1214°C for the Ni-Hf alloy and 1204°C for the Ni-Zr alloy. Partial melting occurred, suggesting that the braze temperatures used were between the solidus and liquidus temperatures of the filler metals. Since eutectic alloys have congruent melting points, this implies that the compositions of the alloys deviated from the eutectic compositions given on the phase diagrams in **Figures 49 and 50**.

Complete melting was eventually achieved at a furnace temperature of 1238°C for both braze alloys. This is 48°C above the equilibrium eutectic temperature for the Ni-Hf alloy, and 68°C above the published Ni-Zr eutectic temperature. It should be noted that three furnace thermocouples were used to control the temperature within the vacuum furnace. All three thermocouples were within ±3°C of the specified temperature of 1238°C during brazing. Two additional load thermocouples placed in contact with the In738 plate gave readings of 1229°C and 1232°C. The real temperature at which the Ni-Hf and Ni-Zr alloys successfully melted and flowed was therefore closer to 1230°C ± 2°C. This is 40°C higher than the published eutectic temperature of the Ni-Hf alloy and 60°C higher than the eutectic temperature of the Ni-Zr alloy.

In order to clarify this discrepancy between the published and measured melting temperatures, the solidus and liquidus temperatures of both braze alloys were determined using Differential Thermal Analysis (DTA), and the chemical compositions were measured using ICP-OE (Inductively Coupled Plasma-Optical Emission) techniques. The results are summarized in Table 9.

Table 9 – Measured chemical compositions (wt.%) of the Ni-Hf and Ni-Zr braze alloys.

Alloy	Ni	Hf	Zr	Co	Cr	Cu	Fe	P	Mn	Si	C
Ni-Hf braze	69.995	28.87	0.70	0.02	0.04	0.01	0.14	0.007	-	0.20	0.018
Ni-Zr braze	86.212	-	13.26	0.02	0.05	0.01	0.18	-	0.01	0.24	0.018

The measured solidus temperature of the Ni-Hf braze alloy was 1176^{o}C and the liquidus temperature 1208^{o}C. The solidus temperature of the Ni-Zr braze was 1163^{o}C and the liquidus temperature 1206^{o}C.

These results indicate that the measured liquidus temperature of the Ni-Hf braze alloy was approximately 18^{o}C higher than the published eutectic temperature, whereas the liquidus of the Ni-Zr alloy was 36^{o}C higher than the equilibrium eutectic temperature. Since the load thermocouples in contact with the In738 plate measured a temperature of 1230^{o}C ± 2^{o}C, the actual brazing temperature was about 22^{o}C to 24^{o}C higher than the measured liquidus temperatures determined by DTA for the Ni-Hf and Ni-Zr braze alloys used in this investigation. Brazing at a temperature ± 25^{o}C higher than the melting point of the braze alloy is within acceptable braze practice.

The observed differences between the published and measured liquidus temperatures can probably be attributed to deviations in chemical composition from the eutectic compositions specified by the phase diagrams (as indicated in **Table 9**). The conclusion was drawn that the Ni, Hf and Zr powders used to make up the braze alloys were not completely pure, leading to contamination of the braze alloys by various residual elements. These elements shifted the compositions of the braze powders away from the eutectic points, leading to higher melting temperatures and incongruent melting points.

3.3.2 Microstructures of the Ni-Hf and Ni-Zr joints after brazing at 1230°C for 40 minutes:

Optical micrographs of the Ni-Hf brazed joint after 40 minutes at 1230^{o}C are shown in **Figures 51 to 53** at various magnifications. **Figure 51** indicates that the Ni-Hf braze alloy melts and flows adequately when processed at 1230^{o}C for 40 minutes, and that a satisfactory bond forms with the In738 substrate material. The braze microstructure, shown in **Figures 52 and 53**, consists of a mixture of coarse and fine dendrites (probably γ), and a second phase that is most likely the Ni_5Hf or Ni_7Hf_2 intermetallic compound.

Figures 54 to 57 display optical micrographs at various magnifications of the Ni-Zr brazed joint after 40 minutes at 1230^{o}C. Like the Ni-Hf braze alloy, the Ni-Zr braze melts and flows satisfactorily when processed at 1230^{o}C for 40 minutes, and an acceptable bond forms with the In738 substrate material (see **Figures 54 and 55**). The braze microstructure, shown in **Figures 55 to 57**, consists of γ dendrites, a Ni_5Zr intermetallic phase, and a γ/γ' flower-shaped eutectic component.

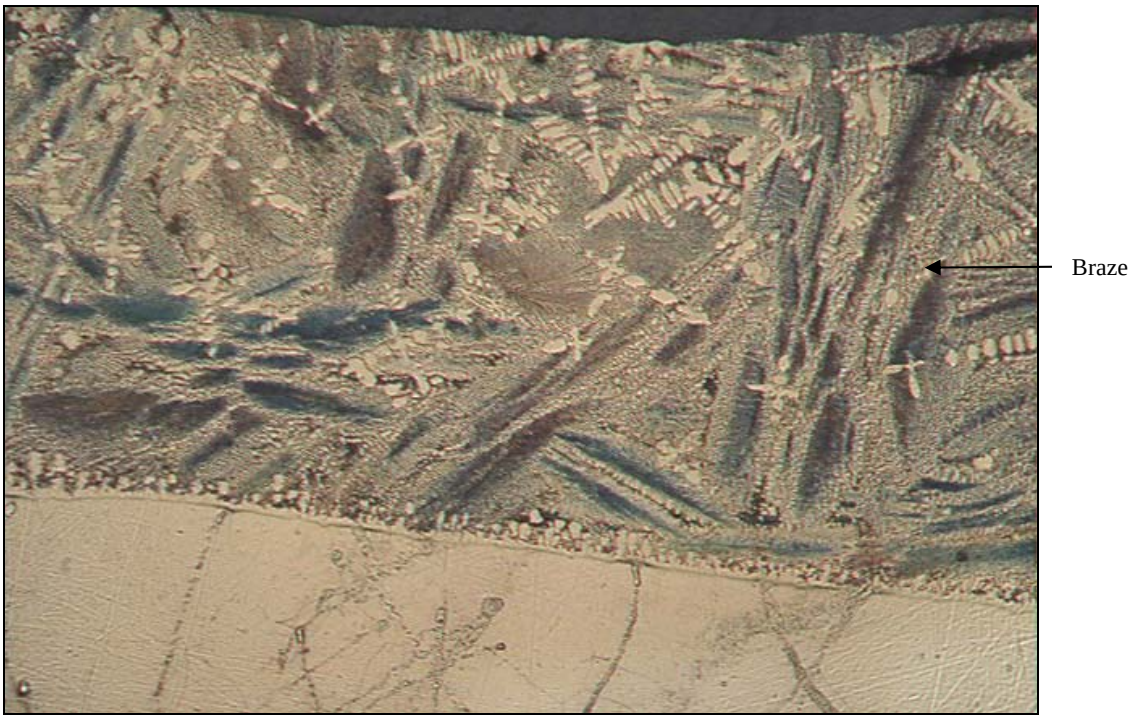

Figure 51 – Optical micrograph of a Ni-Hf brazed joint in In738 parent metal after brazing at 1230°C for 40 minutes. Magnification: 50X.

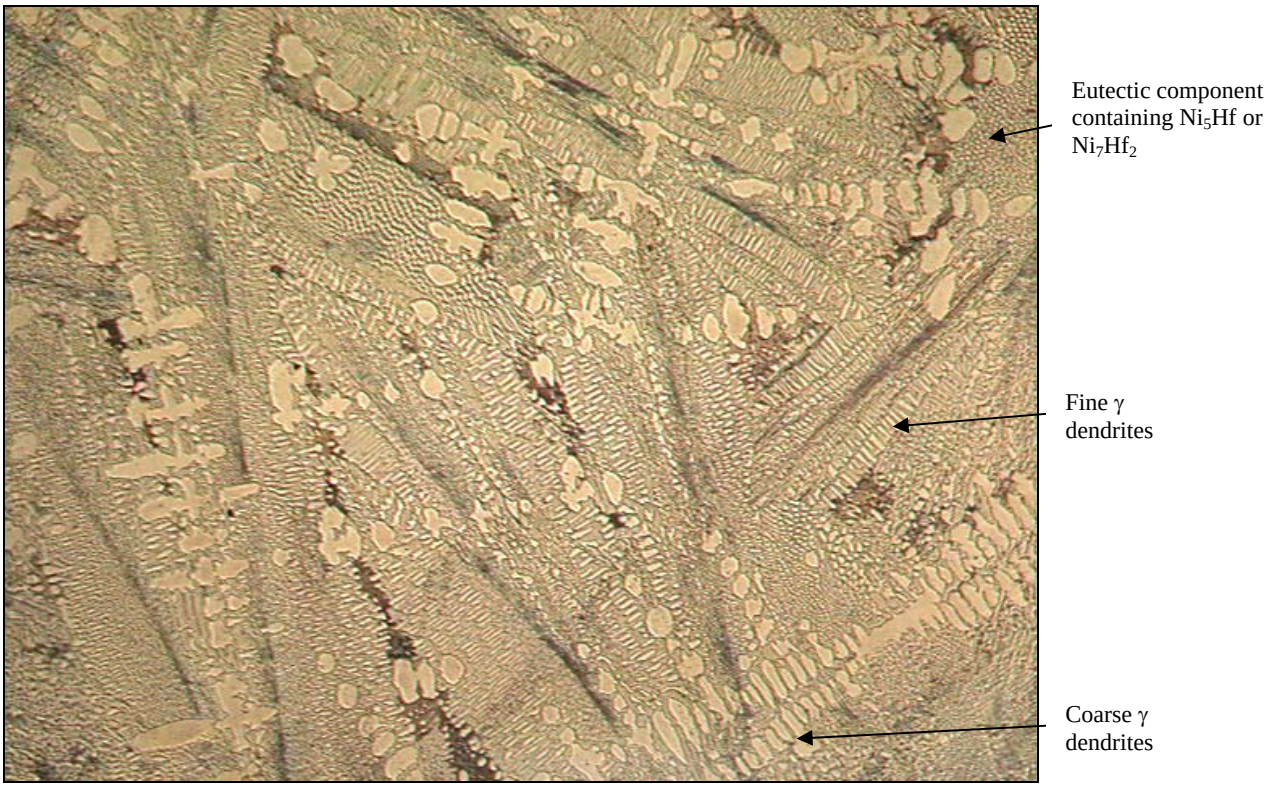

Figure 52 – Optical micrograph of a Ni-Hf brazed joint in In738 parent metal after brazing at 1230°C for 40 minutes. Magnification: 100X.

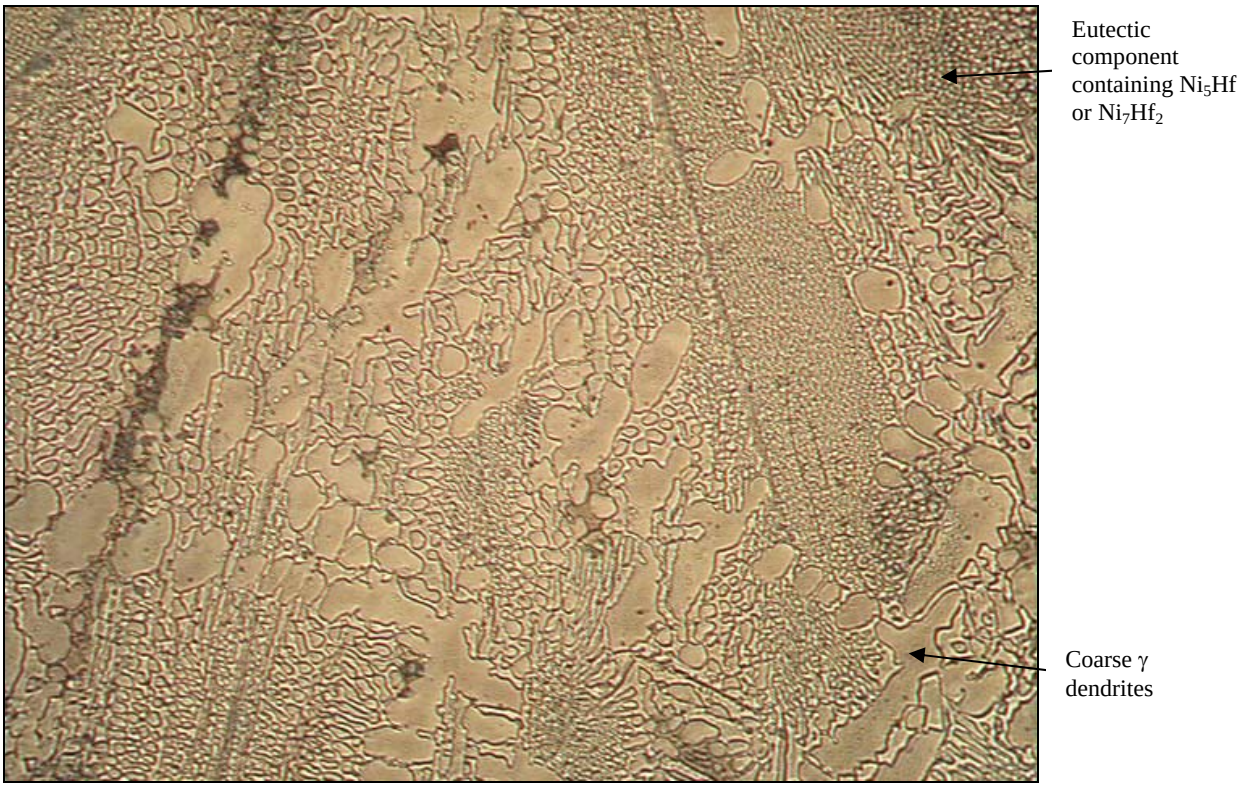

Figure 53 – Optical micrograph of a Ni-Hf brazed joint in In738 parent metal after brazing at 1230°C for 40 minutes. Magnification: 200X.

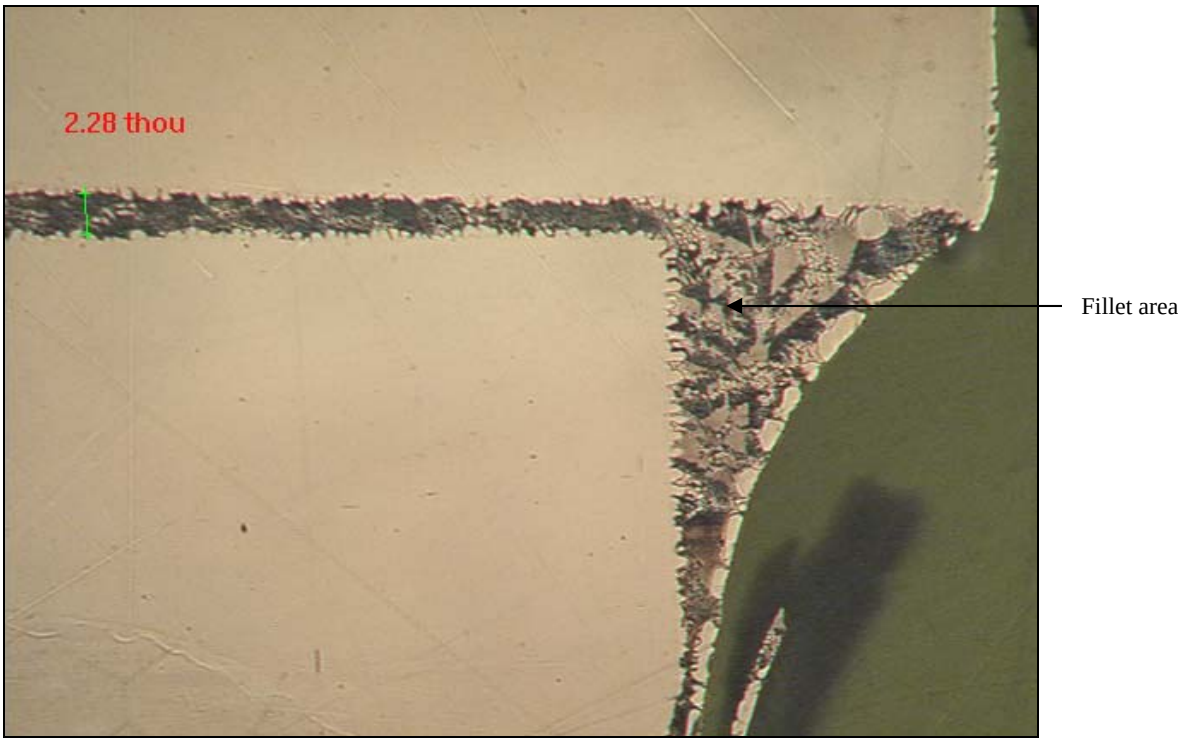

Figure 54 – Optical micrograph of a Ni-Zr brazed joint in In738 parent metal after brazing at 1230°C for 40 minutes. Magnification: 50X.

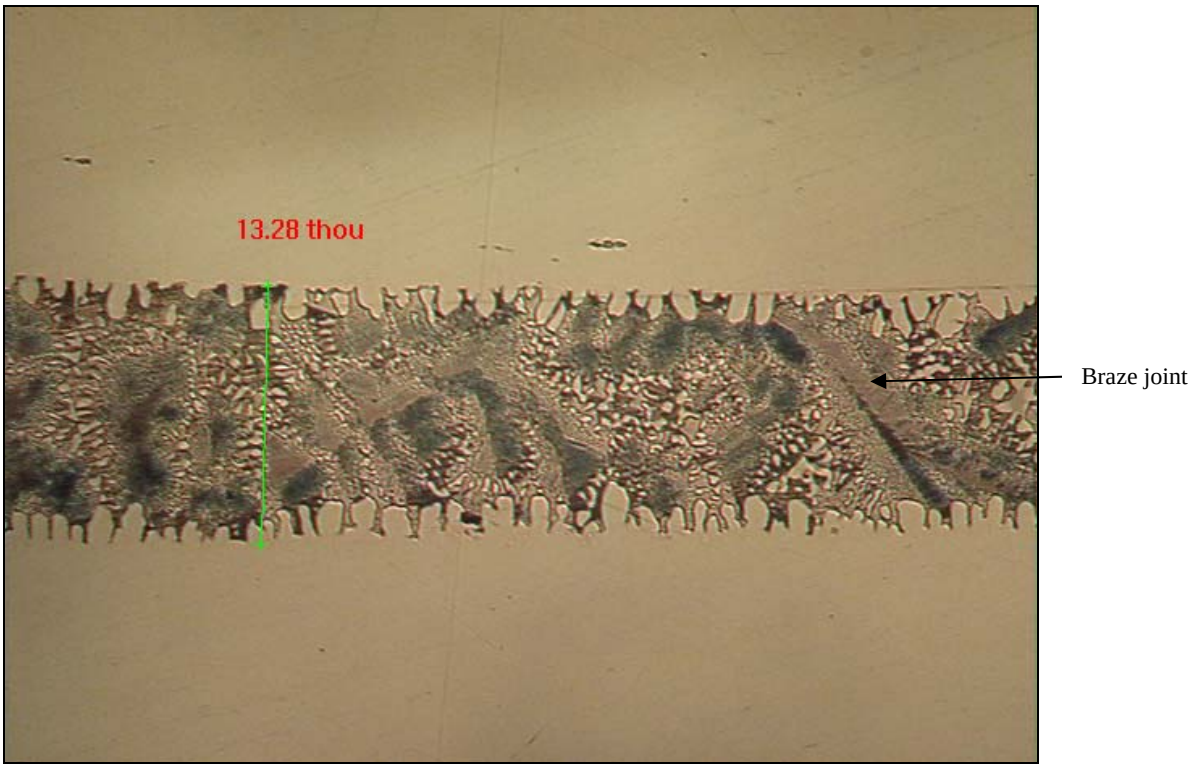

Figure 55 – Optical micrograph of a Ni-Zr brazed joint in In738 parent metal after brazing at 1230°C for 40 minutes. Magnification: 100X.

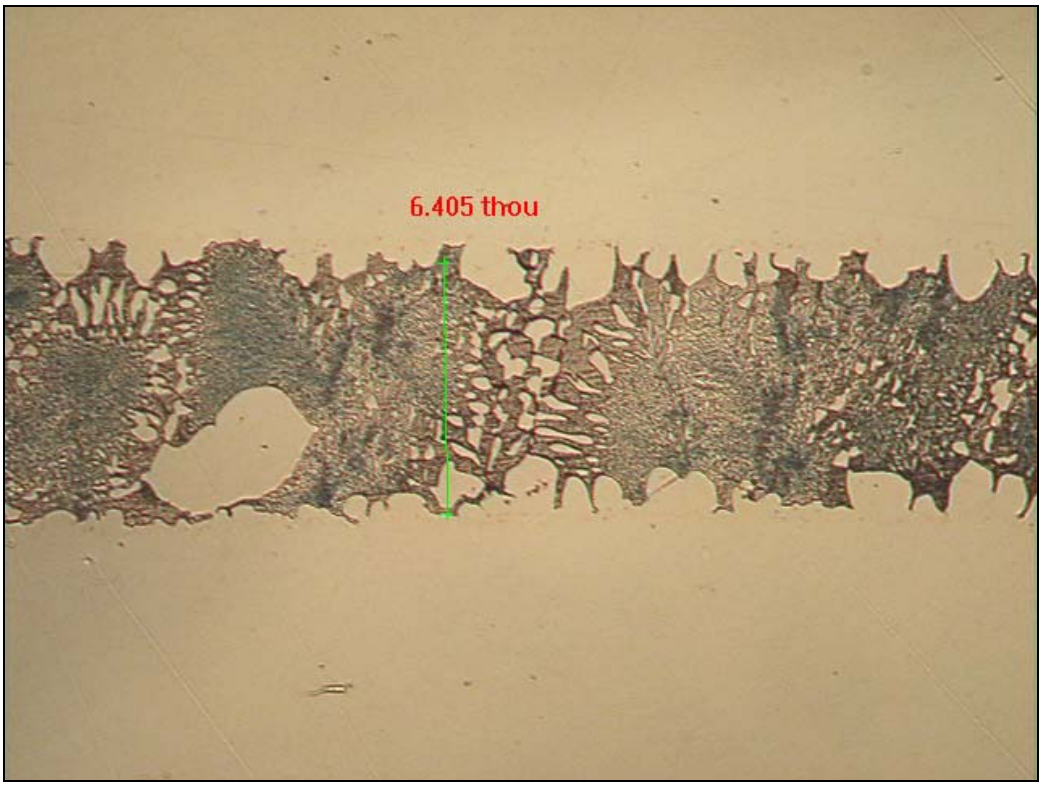

Figure 56 – Optical micrograph of a Ni-Zr brazed joint in In738 parent metal after brazing at 1230°C for 40 minutes. Magnification: 200X.

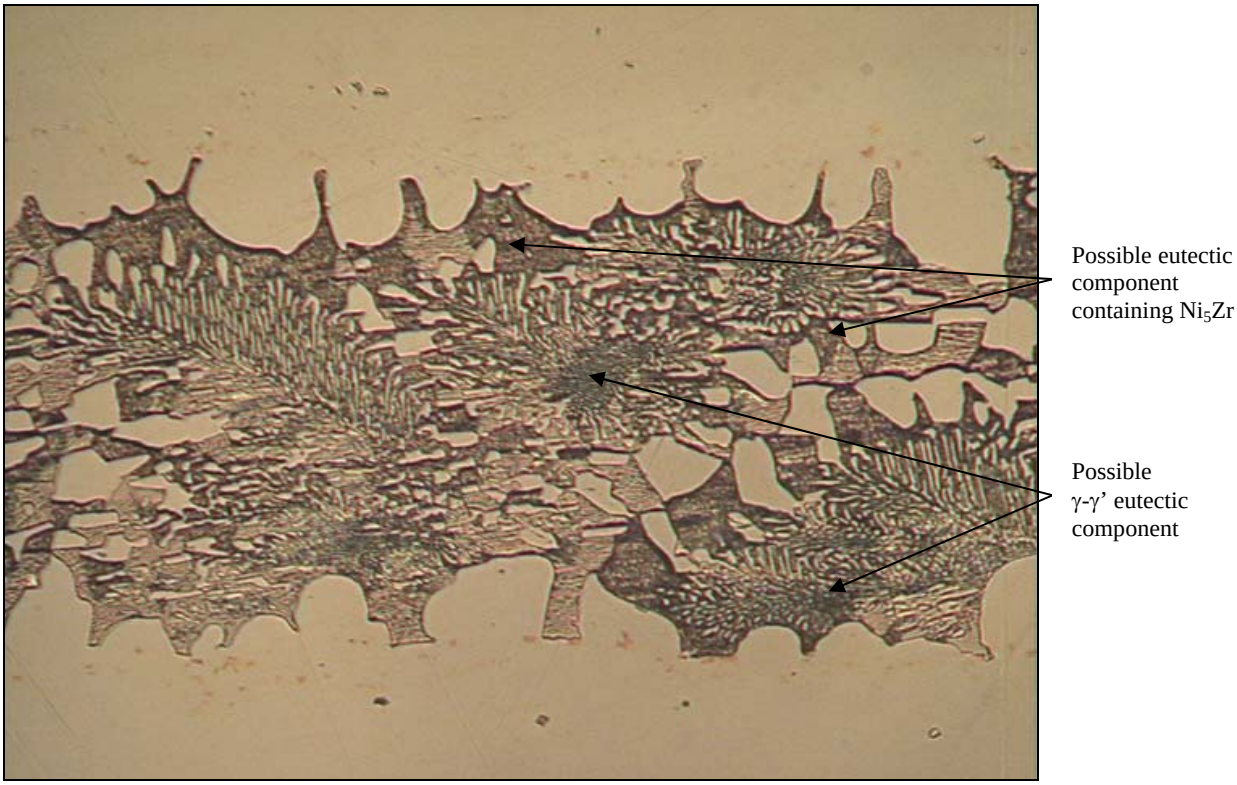

Figure 57 – Optical micrograph of a Ni-Zr brazed joint in In738 parent metal after brazing at 1230°C for 40 minutes. Magnification: 500X.

3.3.3 Microstructures of the Ni-Hf and Ni-Zr joints after brazing at 1230°C for 18 hours:

Optical micrographs of the Ni-Hf braze joint after 18 hours at 1230°C are shown in **Figures 58 to 62** at various magnifications. A brazed joint between two In738 plates is shown in **Figures 58 and 59**. An acceptable fillet area, indicating good braze flow, is evident and an acceptable bond forms with the In738 substrate material. The braze microstructure, shown in **Figures 58 to 61**, consists of mixture of coarse and fine γ dendrites, and a γ/γ' flower-shaped eutectic component that is often observed in Ni-based superalloys. The formation of the γ/γ' eutectic component is probably promoted by the high solubility of Hf in γ' (Hf is a good γ' former). Higher levels of the γ/γ' eutectic component most likely suppress the formation of Hf-rich intermetallic phases in the joint. Nevertheless, the Ni_5Hf or Ni_7Hf_2 intermetallic phase is evident, as shown in **Figure 62**.

A Ni-Zr brazed joint between two In738 plates is shown at various magnifications in **Figures 63 to 66** after brazing at 1230°C for 18 hours. Adequate bonding of the braze alloy to the In738 substrate is evident from **Figures 63 and 64**. The braze microstructure, shown in **Figures 63 to 66**, consists of a mixture of coarse and fine γ dendrites and a Ni_5Zr intermetallic phase.

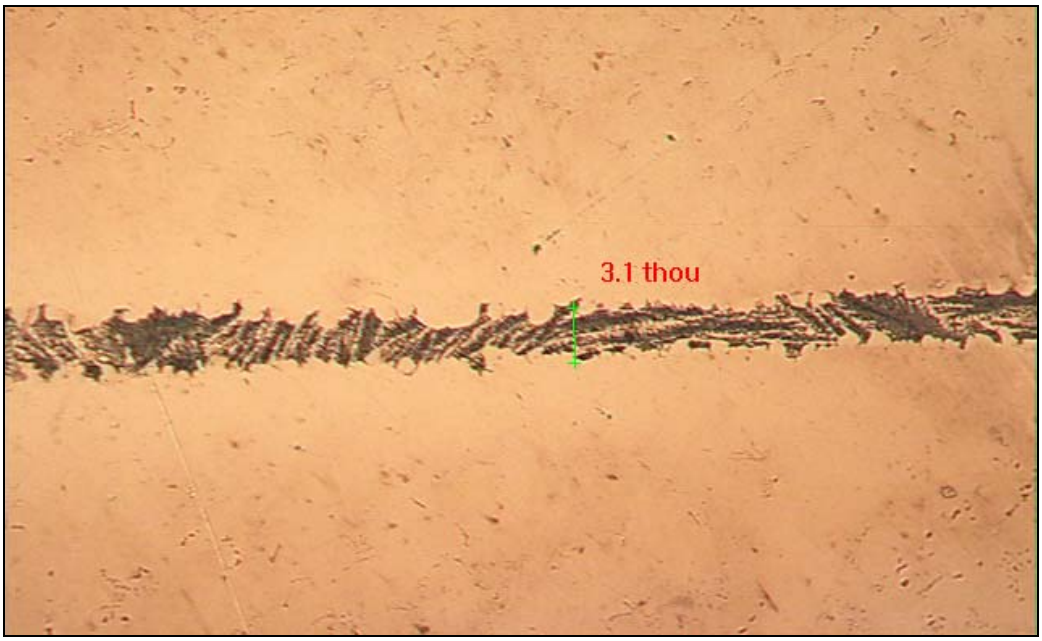

Figure 58 – Optical micrograph of a Ni-Hf brazed joint in In738 parent metal after brazing at 1230°C for 18 hours. Magnification: 50X.

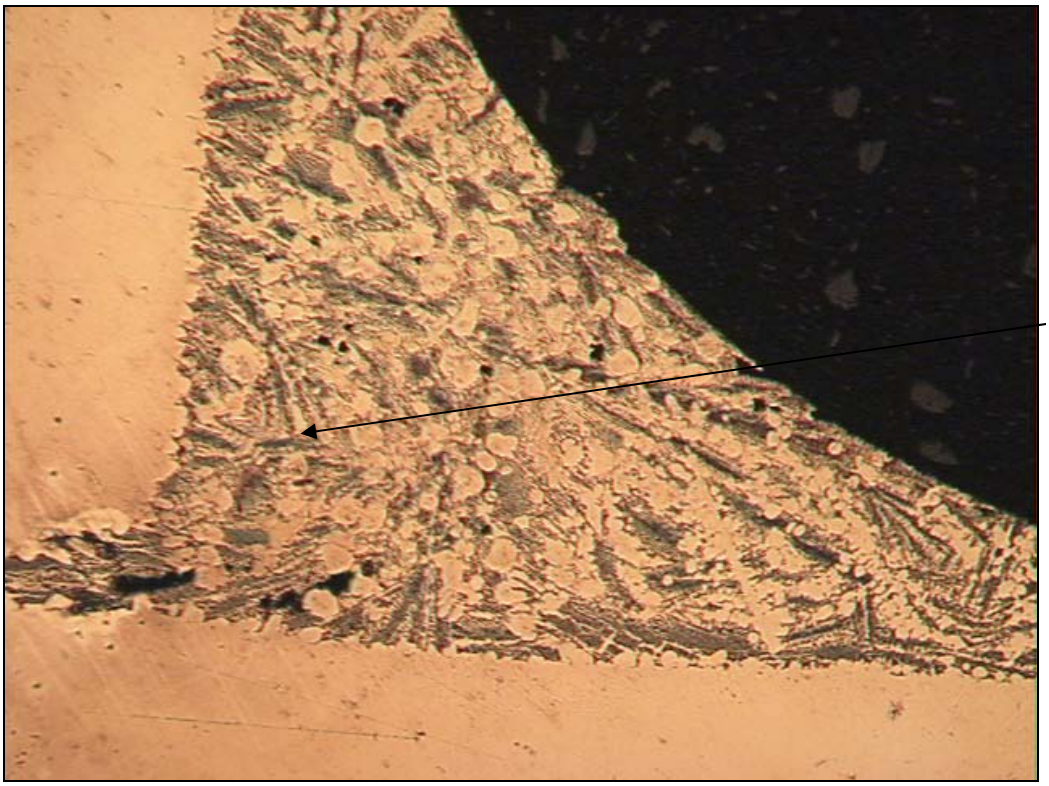

Figure 59 – Optical micrograph of a Ni-Hf brazed joint in In738 parent metal after brazing at 1230°C for 18 hours. Magnification: 50X.

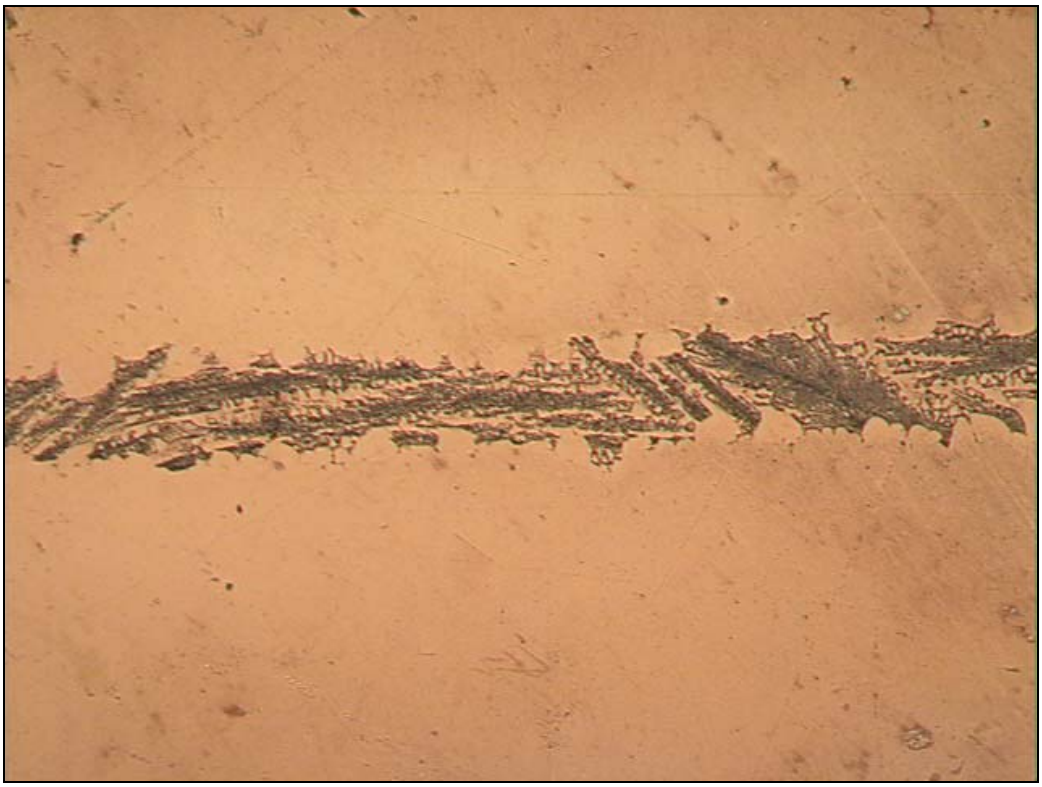

Figure 60 – Optical micrograph of a Ni-Hf brazed joint in In738 parent metal after brazing at 1230°C for 18 hours. Magnification: 100X.

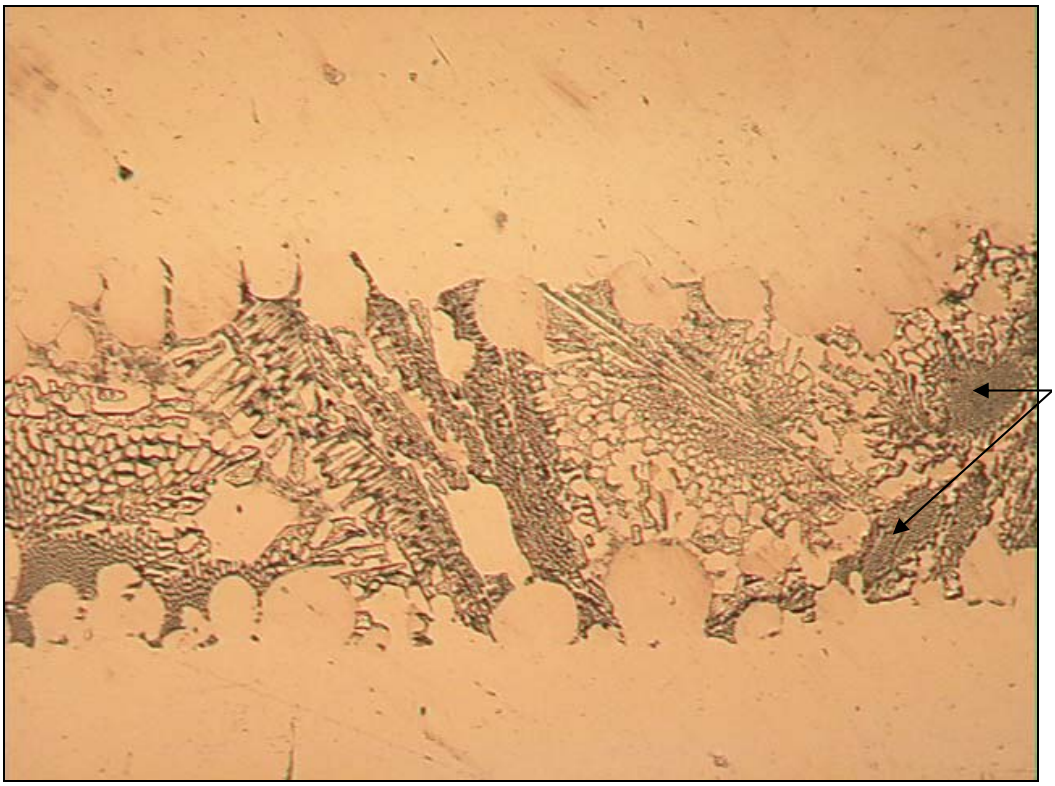

Figure 61 – Optical micrograph of a Ni-Hf brazed joint in In738 parent metal after brazing at 1230°C for 18 hours. Magnification: 200X.

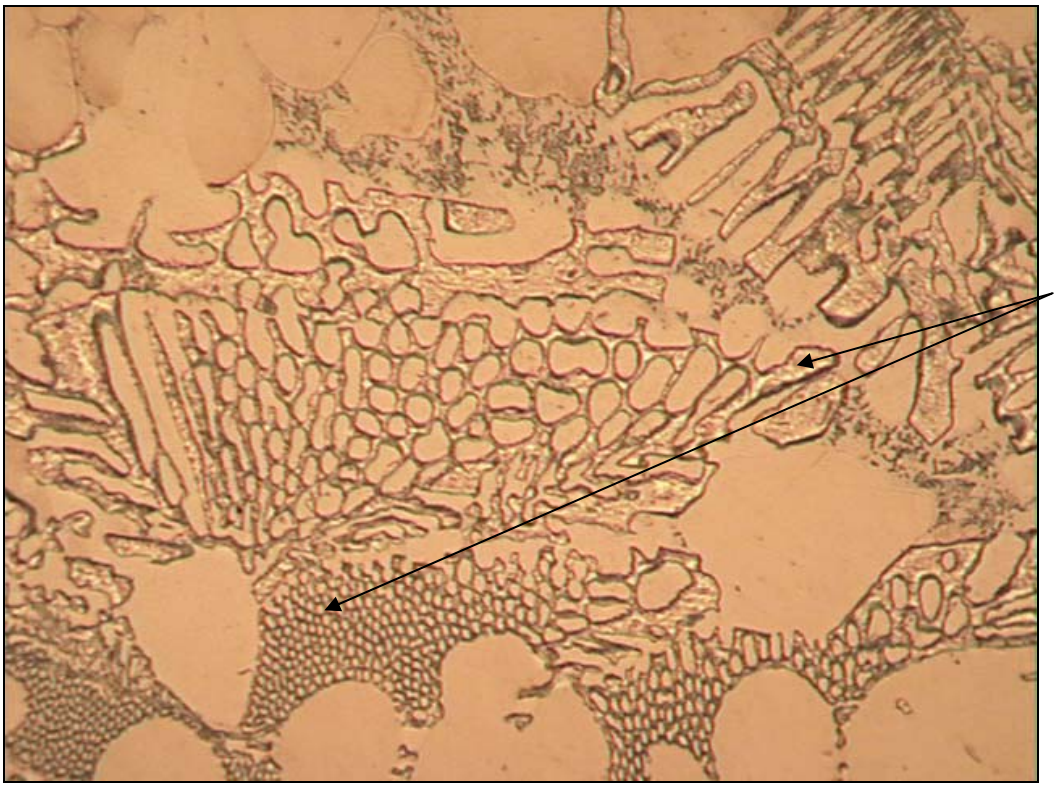

Figure 62 – Optical micrograph of a Ni-Hf brazed joint in In738 parent metal after brazing at 1230°C for 18 hours. Magnification: 500X.

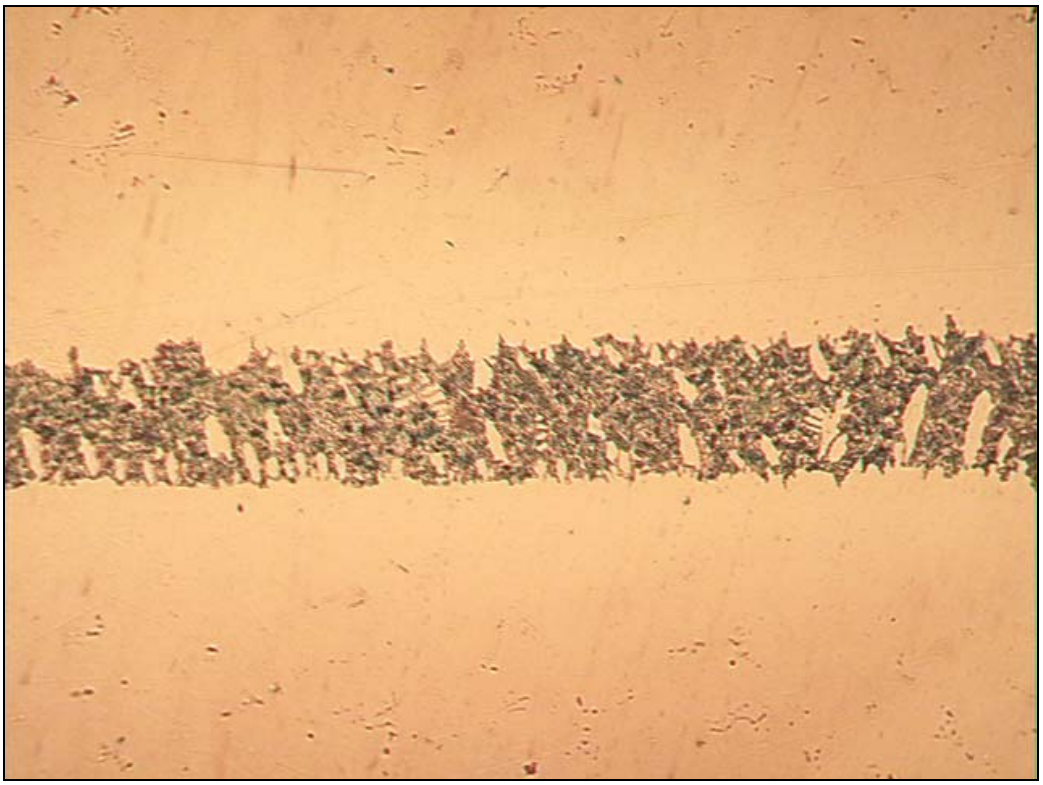

Figure 63 – Optical micrograph of a Ni-Zr brazed joint in In738 parent metal after brazing at 1230°C for 18 hours. Magnification: 50X.

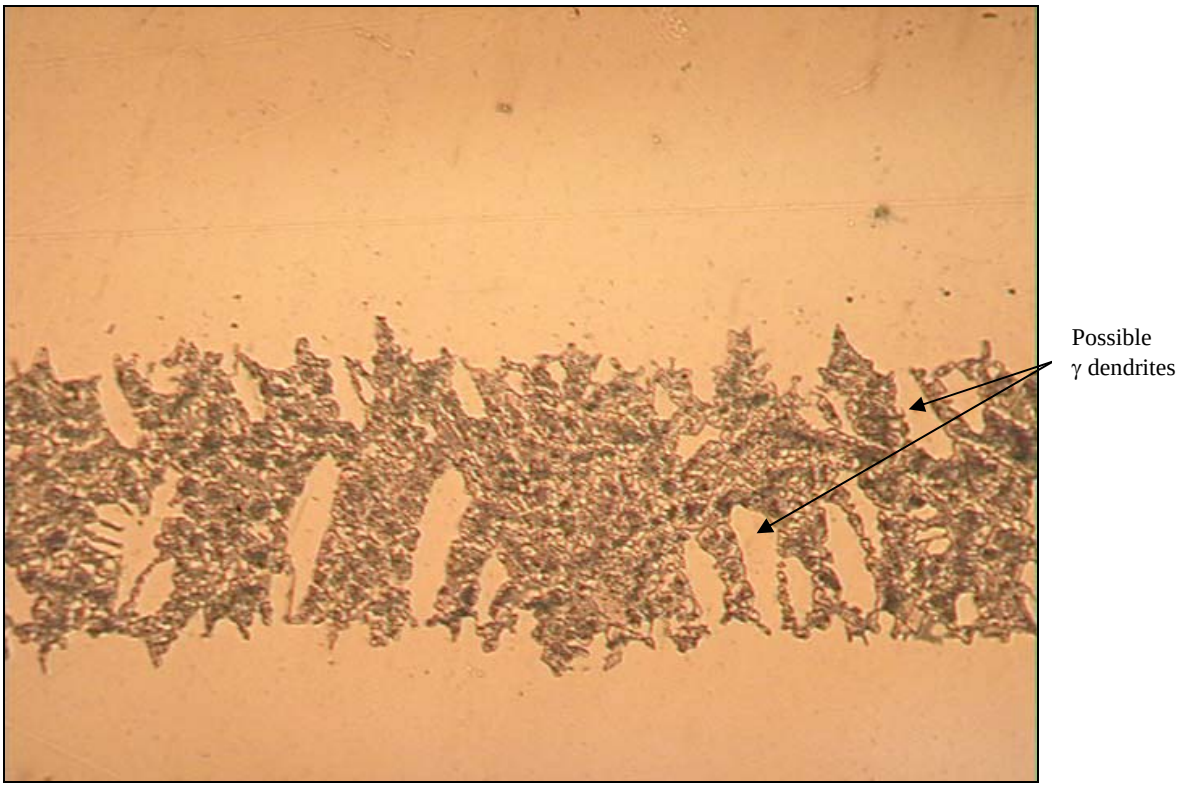

Figure 64 – Optical micrograph of a Ni-Zr brazed joint in In738 parent metal after brazing at 1230°C for 18 hours. Magnification: 100X.

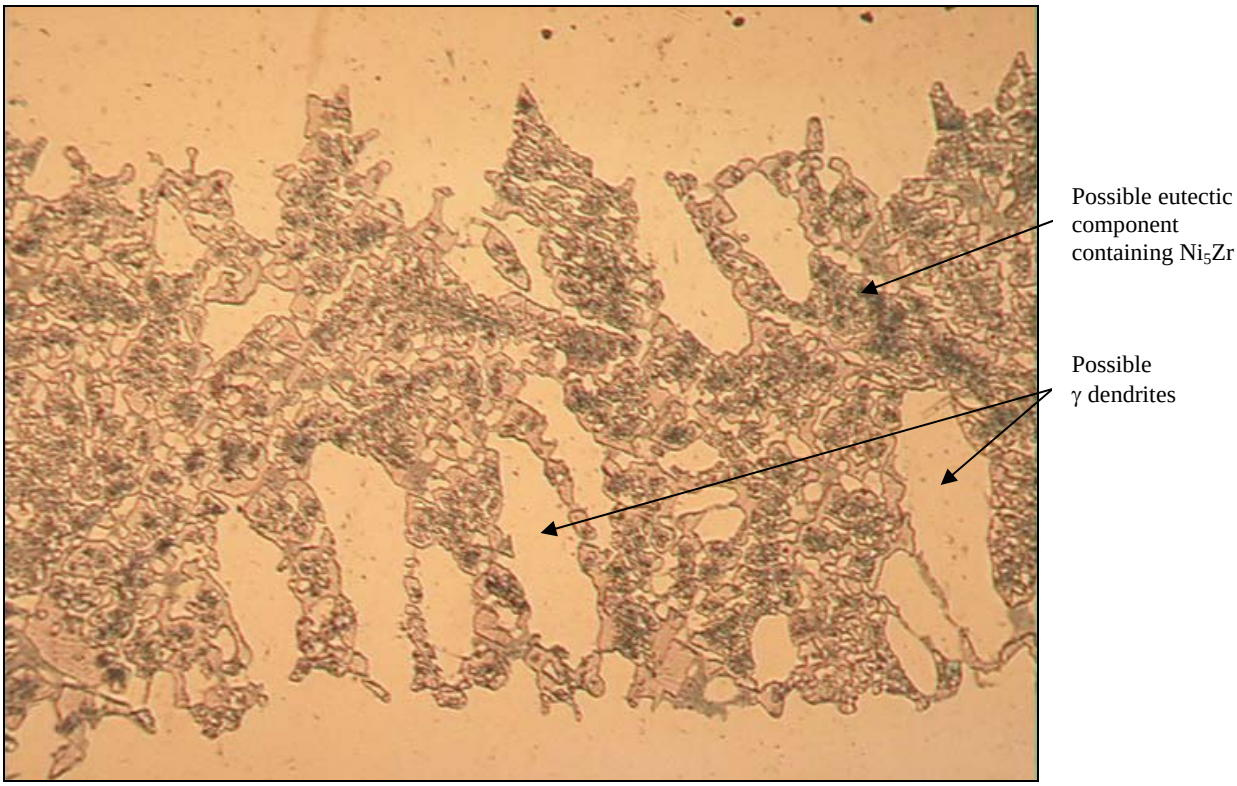

Figure 65 – Optical micrograph of a Ni-Zr brazed joint in In738 parent metal after brazing at 1230°C for 18 hours. Magnification: 200X.

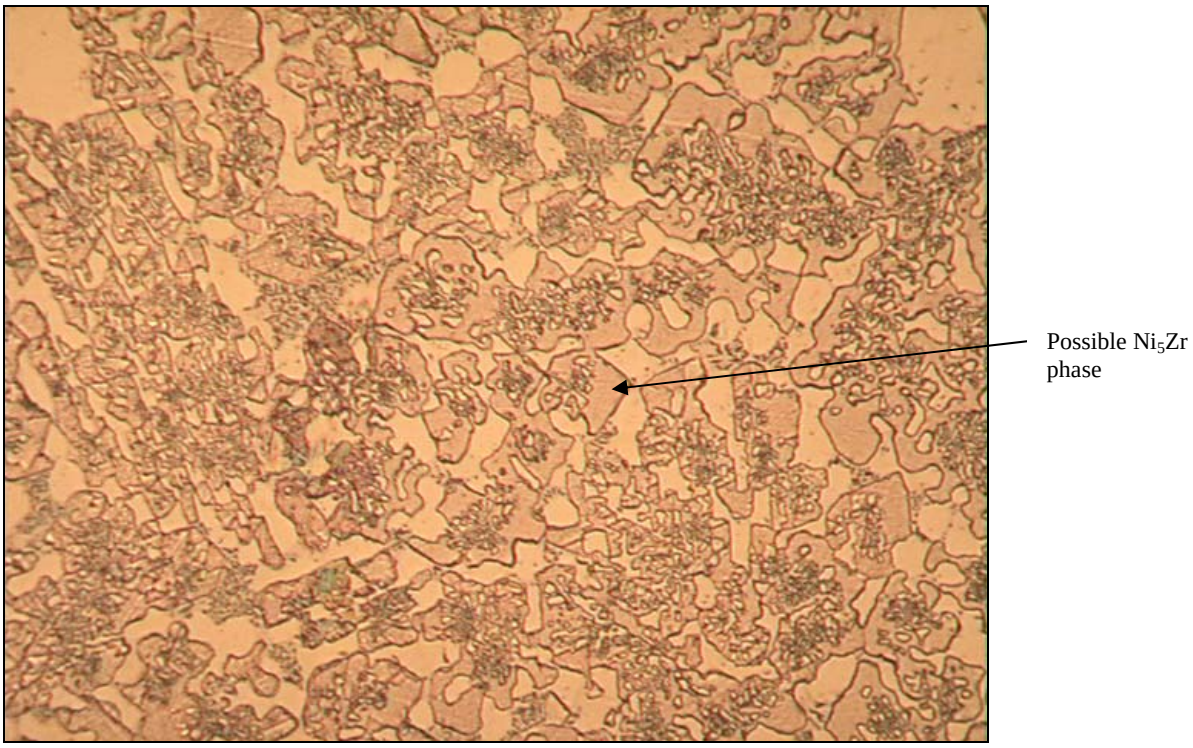

Figure 66 – Optical micrograph of a Ni-Zr brazed joint in In738 parent metal after brazing at 1230°C for 18 hours. Magnification: 500X.

A SEM micrograph of the Ni-Hf joint brazed at 1230°C for 18 hours is shown in **Figure 67.** SEM-EDS analysis was performed on the two phases highlighted by the arrows in **Figure 67**. One phase was arbitrarily labelled "grain boundary particle". The energy dispersive x-ray analysis revealed a composition of 78.72Ni-5.97Co-4.47Cr-4.00Al-2.82W-2.53Fe-0.53Mo-0.38Ti (wt.%) for this phase, identifying it as the γ phase. The second phase was arbitrarily designated "grain boundary film", and had a composition of 49.21Ni-45.74Hf-2.32W-1.94Co-0.37Cr-0.28Al-0.14Ti. The binary Ni-Hf phase diagram, shown in **Figure 49**, indicates that the Ni_7Hf_2 intermetallic phase contains 46.5% Hf, whereas the Ni_5Hf phase has a nominal Hf content of 37.9% Hf. The "grain boundary film" phase was therefore provisionally identified as the Ni_7Hf_2 intermetallic compound. The SEM-EDS analysis also indicates that small amounts of W, Co, Cr, Al and Ti are soluble in this phase. The presence of coarse γ dendrites in the Ni-Hf braze alloy suggests that the alloy may be slightly hypoeutectic, resulting in the formation of a proeutectic γ phase on solidification. The existence of Ni_7Hf_2 in the braze alloy was, however, unexpected, since the phase diagram (**Figure 49**) predicts a γ-Ni_5Hf eutectic component. It is not clear why the formation of the Ni_5Hf intermetallic compound was suppressed on solidification. The cooling rate after brazing may have been too fast to achieve true equilibrium, or the published phase diagram may be incorrect. In-depth investigation into the cause of this deviation from the predictions of the phase diagram falls outside the scope of this experiment and further speculation is therefore not justified at this time.

Figure 68 displays a SEM micrograph of the Ni-Zr joint brazed at 1230°C for 18 hours. Two phases, highlighted by the arrows in **Figure 68**, were analyzed. The phase arbitrarily labelled "grain boundary particle" had a composition of 78.82Ni-9.00Zr-3.08Co-2.97Cr-3.05Al-1.24Fe-1.57Mo-0.26Ti (wt.%) and was identified as the γ phase. This braze alloy also appears to be slightly hypoeutectic, forming a proeutectic γ phase on solidification. The

second phase, arbitrarily labelled "grain boundary film", had a composition of 71.24Ni-24.91Zr-1.45W-1.47Co-0.57Cr-0.38Mo. According to the Ni-Zr phase diagram shown in **Figure 50**, the Ni_5Zr phase contains between 21.32 and 25.95% Zr, suggesting that the phase labelled "grain boundary film" is the Ni_5Zr intermetallic compound that forms as part of the γ-Ni_5Zr eutectic component. Small amounts of W, Co, Cr and Mo are soluble in this phase.

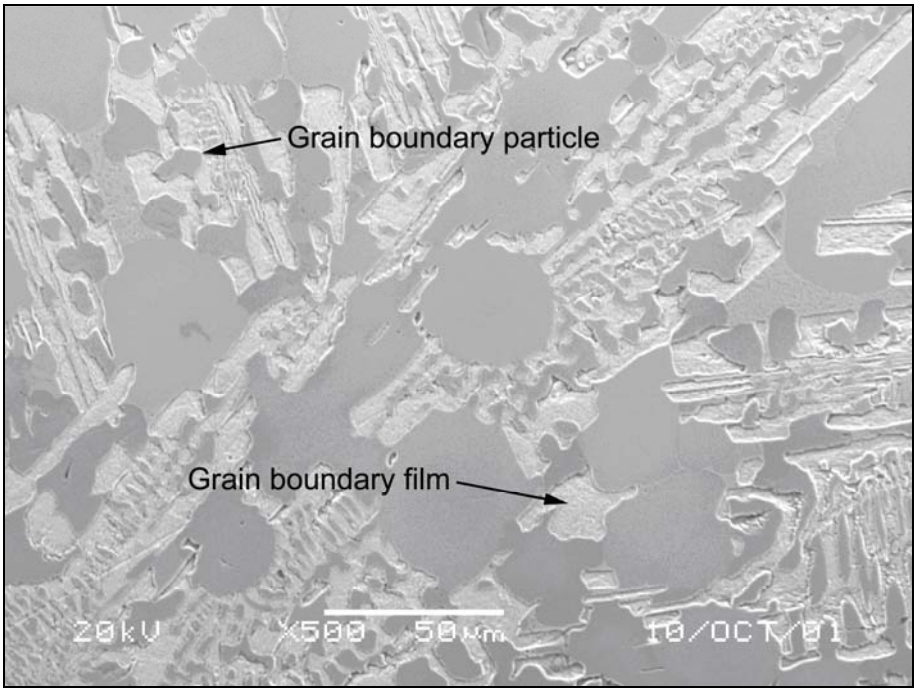

Figure 67 – SEM micrograph of the Ni-Hf braze, showing the phases identified as γ (labelled "grain boundary particle") and Ni_7Hf_2 (labelled "grain boundary film").

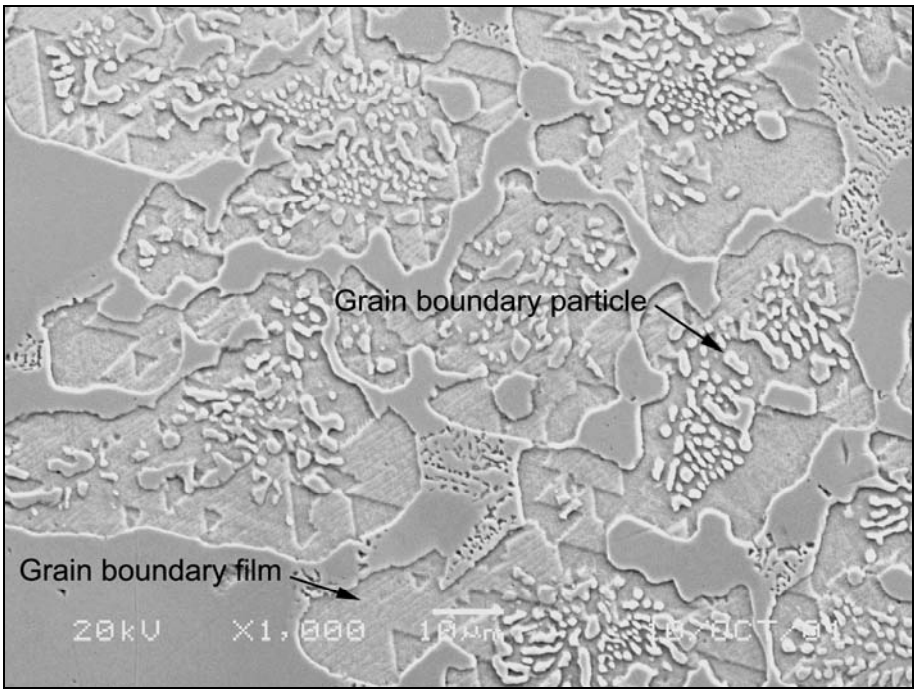

Figure 68 – SEM micrograph of the Ni-Zr braze, showing the phases identified as γ (labelled "grain boundary particle") and Ni_5Zr (labelled "grain boundary film").

3.4) Conclusions

- The eutectic Ni-Hf and Ni-Zr braze alloys did not melt at the equilibrium eutectic temperatures predicted by the binary phase diagrams. This was attributed to a shift in chemical composition away from the eutectic point due to contamination of the powders used to mix the braze alloys. The brazing temperature for both alloys was optimized at $1230^{o}C \pm 2^{o}C$. This temperature is approximately 25°C higher than the measured liquidus temperatures of the alloys.

- The Ni-Hf and Ni-Zr braze alloys exhibited good flow and wetting of the substrate at a brazing temperature of $1230^{o}C$. Narrow gaps in In738 parent metal can be repaired successfully using either of the novel braze alloys. The joints produced at $1230^{o}C$ appeared to consist of:

    1) coarse and fine γ dendrites,
    2) a flower-shaped γ-γ' eutectic component (in the Ni-Hf joints), and
    3) a γ-Ni_7Hf_2 or γ-Ni_5Zr eutectic component.

- The mechanical properties of the joints were not evaluated during the course of Experiment 1. Based on the chemistry (simple binary eutectic Ni-Hf or Ni-Zr alloys), it is reasonable to assume that wide joints with clearances greater than 0.10 mm will not exhibit strength levels approaching those of the base metal. In order to determine whether high strength joints can be produced using the novel braze alloys, liquid phase diffusion bonds were produced using the Ni-Hf and Ni-Zr braze powders in combination with Ni-base superalloy powder within the joint. The results are presented in Chapter 4.